Colloid Polym Sci (2015) 293:2137–2146
DOI 10.1007/s00396-015-3602-z

ORIGINAL CONTRIBUTION

Drying dissipative patterns of aqueous solution of poly (methacrylic acid) and its salt neutralized half

Tsuneo Okubo[1] · **Akira Hagiwara**[2] · **Hiromi Kitano**[2] · **Shinya Takahashi**[3] · **Akira Tsuchida**[3]

Received: 11 March 2015 / Revised: 5 April 2015 / Accepted: 14 April 2015 / Published online: 28 April 2015

Abstract Drying patterns of poly(methacrylic acid) (HPMA) and its salt neutralized half with sodium hydroxide (NaHPMA) were studied on a cover glass, a watch glass, and a glass dish. The patterns of HPMA and NaHPMA are compared with the previous observation of sodium salt of poly(methacrylic acid), NaPMA (Okubo et al. Colloid Polym Sci 287:1155–1165, 2009). HPMA and especially NaHPMA are hygroscopic, and only the macroscopic patterns were observed. However, microscopic patterns were not observed clearly especially for NaHPMA in the room atmosphere. The hygroscopy of the dried films was in the order NaPMA < HPMA < NaHPMA. Broad rings of HPMA formed only at the outside edge irrespective of polymer concentration. Simplified laurel crown-like patterns appeared on a cover glass, which supports the strong solute–substrate affinity. On the other hand, the broad ring size of NaHPMA decreased sharply at the lower polymer concentrations than the critical concentration, m^*. The results of NaHPMA support that both the inter-solutes and solute–substrate affinity are rather weak, and the pattern size was determined with the *excluded volume effects*. Sharpness parameter, S, of the broad rings was in the order HPMA > NaHPMA > NaPMA. The magnitude of S values of NaPMA was similar to that of poly(ethylene glycol) (PEG). HPMA, NaHPMA, and NaPMA were grouped into E, A, and A, respectively, among six groups of solutes A to F.

Keywords Poly(methacrylic acid) (HPMA) · Laurel crown pattern · Drying pattern · Broad ring pattern · Hygroscopic polymer

✉ Tsuneo Okubo
okubotsu@ybb.ne.jp

[1] Institute for Colloidal Organization, Hatoyama 3-1-112, Uji, Kyoto 611-0012, Japan

[2] Department of Applied Chemistry, Graduate School of Science and Engineering, University of Toyama, Toyama 930-8555, Japan

[3] Department of Applied Chemistry, Faculty of Engineering, Gifu University, Yanagido 1, Gifu 501-1193, Japan

Introduction

Most structural patterns in nature form via self-organization accompanied with the *dissipation* of free energy and in the non-equilibrium state. In order to know the mechanisms of the dissipative *self-organization* of the simple model systems instead of the much complex nature itself, the authors have studied the *convectional*, *sedimentation*, and *drying* dissipative patterns during the course of drying colloidal suspensions and solutions as systematically as possible, though the three kinds of patterns are correlated strongly and overlapped to each other [1–4]. The drying patterns form cooperatively among the processes of (i) the *wetting* of suspensions and solutions with substrate surface, (ii) the *evaporation* of solvent, (iii) the *convection* of solvents and solutes, (iv) the *sedimentation* of solutes, and (v) the *solidification* during the course of dryness.

It should be further noted that *information* on the *size*, *shape*, *conformation*, and/or *flexibility* of particles and polymers, for example, is transformed cooperatively and further accompanied with the *amplification* and *selection* processes toward the drying patterns [4–7].

Typical convectional patterns are the Benard cell [8, 9], the *hexagonal* circulating pattern, and the Terada cell [10–13], the *spoke lines* spreading whole the liquid surface accompanied with the huge number of *cell convections* in the normal direction of the spoke lines. Recently, whole processes of the

convectional patterns have been studied experimentally [14–21]. These convectional patterns were observed often in the intermediate and even final step of the drying patterns [11–19], which supports the cooperation of the five processes, wetting, evaporation, convection, sedimentation, and solidification during the course of dryness.

Sedimentary patterns have been studied in detail, for the first time, in the author's laboratory [15–29]. Several types of the sedimentary patterns, the *broad rings*, for example, formed already in suspension state. In most cases, the sedimentary particles are suspended in a vessel by the *electrical double layers* formed around the particles and moved always by the balancing of the force fields between the convectional flow and the gravitational sedimentation during the course of thermal diffusion. Dynamic *clusters* and *bundle*-like sedimentary patterns formed cooperatively from the convectional structures.

The final *solidified* drying patterns have been studied for many kinds of solutes, i.e., colloidal particles, linear-type synthetic and biological polyelectrolytes, water-soluble neutral polymers, ionic and non-ionic surfactants, gels, colloidal polymer-complex particles, and dyes, for example, by many researchers hitherto [1–4, 14–49]. The macroscopic *broad ring* and *spoke-like* patterns formed frequently. Microscopic fractal patterns such as branch-, arc-, block-, star-, cross-, string-, earthworm-like, and others were often observed especially in the central and thin area.

Drying dissipative patterns of poly(ethylene glycol) (PEG) have been studied on the macroscopic and microscopic scales [41]. The *dissipative crystalline structures* of *hedrite* and *spherulite* were observed on a cover glass, a watch glass, and a glass dish. Lamellae formed along the ring patterns especially at high concentrations and molecular weights of polymer. The coupled patterns of the spherulites and the lamellae were formed especially in a watch glass. Dissipative crystalline structures such as hedrites and spherulites were also observed clearly in the dried film of sodium salt of poly(methacrylic acid) (NaPMA) [42]. Several important findings on the drying patterns of NaPMA were obtained. Firstly, *spherulite* and *hedrite* dissipative crystals were observed in the dried patterns. The crystalline structures changed from hedrites to spherulites as polymer concentration increased. Secondarily, the coupled structures of the spherulites and the broad rings were observed for NaPMA at the outside edge of the broad ring. However, the coupled crystalline structures of the lamellae and the spherulites, which were observed for PEG [41], were not observed clearly for NaPMA system. Thirdly, size of the broad ring at the outside edge of the dried film increased sharply as polymer concentration increased in the concentration range below the critical concentration m^*. Morphological change of the crystal structures has been observed on the drying patterns of biopolymers, i.e., sodium poly(α, L-glutamate) (NaPGA) [43], poly(L-lysine hydrobromide) (PLLHBr) [44], α-, β-, and γ-cyclodextrins [45], sodium salt of deoxyribonucleic acid (NaDNA) [46], potassium salt of poly(riboadenylic acid) (KPolyA), and others [47–49].

In this work, macroscopic and microscopic drying patterns of poly(methacrylic acid) (HPMA) and its sodium salt neutralized half (NaHPMA) were studied in order to clarify the neutralization effects on the drying patterns.

Experimental

Materials

HPMA was synthesized for 24 h at 60 °C from the mixtures of α,α′-azobisisobutynitrile (AIBN) (58.2 mg), methanol (35.4 ml), 2-mercaptoethanol (0.125 ml), and methacrylic acid (3.0 ml). The mixture was purged with nitrogen gas for 30 min before polymerization treatment. Chain transfer agent of 2-mercaptoethanol was used in the free radical polymerization to obtain the HPMA sample of narrow molecular weight distribution. The product HPMA was dialyzed with the membrane film (3,500 of molecular weight cutoff (MWCO), Spectra/Por®, regenerated cellulose, Spectrum Laboratories, Inc., Rancho Dominguez, CA). Poly(methacrylic acid) neutralized half, NaHPMA, was obtained by the neutralization of the part of HPMA with half of the equivalent amount of the aqueous solution of sodium hydroxide. Number average (Mn) and weight average molecular weights (Mw) of HPMA and NaPMA measured on a gel permeation chromatography (Shimadzu LC-10AD pump, Kyoto and Waters R401 Differential refractometer) were 9,520 and 12,900 and 9,760 and 14,200, respectively. The ratios Mw/Mn were 1.35 and 1.45 for HPMA and NaPMA, respectively. The column used was Wakobeads G-30 (Wako Chemicals Co., Osaka), and the standard samples were Pullulan from Showa Denko Co. Mobile phase was 0.1 M aqueous phosphate buffer (pH=6.8). Flow rate was 0.4 ml/min. Tacticity of the HPMA was discussed by 1H-NMR measurements. The triad compositions of rr (*syndiotactic*), mr (*heterotactic*), and mm (*isotactic*) were evaluated as 64:31:5, which supports the fact that HPMA obtained in this work is mainly *atactic* but containing a small amount of *syndiotactic* configuration. Salt neutralized half with NaOH (NaHPMA) (degree of neutralization=0.5) was obtained by adding 0.1 M NaOH aqueous solution into the HPMA solution. The water used for the sample preparation was purified by a

Milli-Q reagent grade system (Milli-RO5 plus and Milli-Q plus, Millipore, Bedford, MA).

Observation of the dissipative structures

Aliquot (0.1 ml) of the aqueous solution of HPMA or NaHPMA was carefully and gently placed onto a micro cover glass (30 mm×30 mm, no. 1, thickness 0.12 to 0.17 mm, Matsunami Glass, Kishiwada, Osaka) set in a plastic dish (type NH-52, 52 mm in diameter, 8 mm in depth, As One Co., Tokyo). The cover glass was used without further rinse. Four millimeters of the solution was set on a medium watch glass (70 mm, TOP Co., Tokyo). Five milliliters of the solution was put into a medium glass dish (42 mm in inner diameter and 15 mm in height, code 305-02, TOP Co.). The disposable serological pipettes (1 and 10 ml, Corning Lab. Sci., Co.) were used for the putting the solution on the substrates. The patterns during the course of dryness were observed for the solutions on a desk covered with a black plastic sheet. The room temperature was regulated at 25 °C. Humidity of the room was not regulated and was between 45 and 60 %.

Macroscopic patterns were observed on a Canon EOS 10 D digital camera with a macro-lens (EF 50 mm, f= 2.5) plus a life size converter EF or a zoom lens (Canon, EF 28–70 mm, 1:2.8) on a cover glass and a medium glass dish or a medium watch glass, respectively. Microscopic drying patterns were observed with a metallurgical microscope (PME-3, Olympus Co., Tokyo). Polarizing microscopic pictures of HPMA were taken on a Shimadzu polarizing microscope (type Kalnew 53255, Shimadzu, Kyoto) with a CCD camera (type TNC4604J, Kenis Ltd, Osaka).

Results and discussion

Macroscopic drying patterns of HPMA and NaHPMA solutions

Figure 1 shows the typical macroscopic drying patterns of HPMA solutions at the concentrations from 0.0067 monoM (d) to 0.1 monoM (a). Frame size of the pictures a to d is 14 mm×14 mm. The broad ring patterns were recognized irrespective of the initial polymer

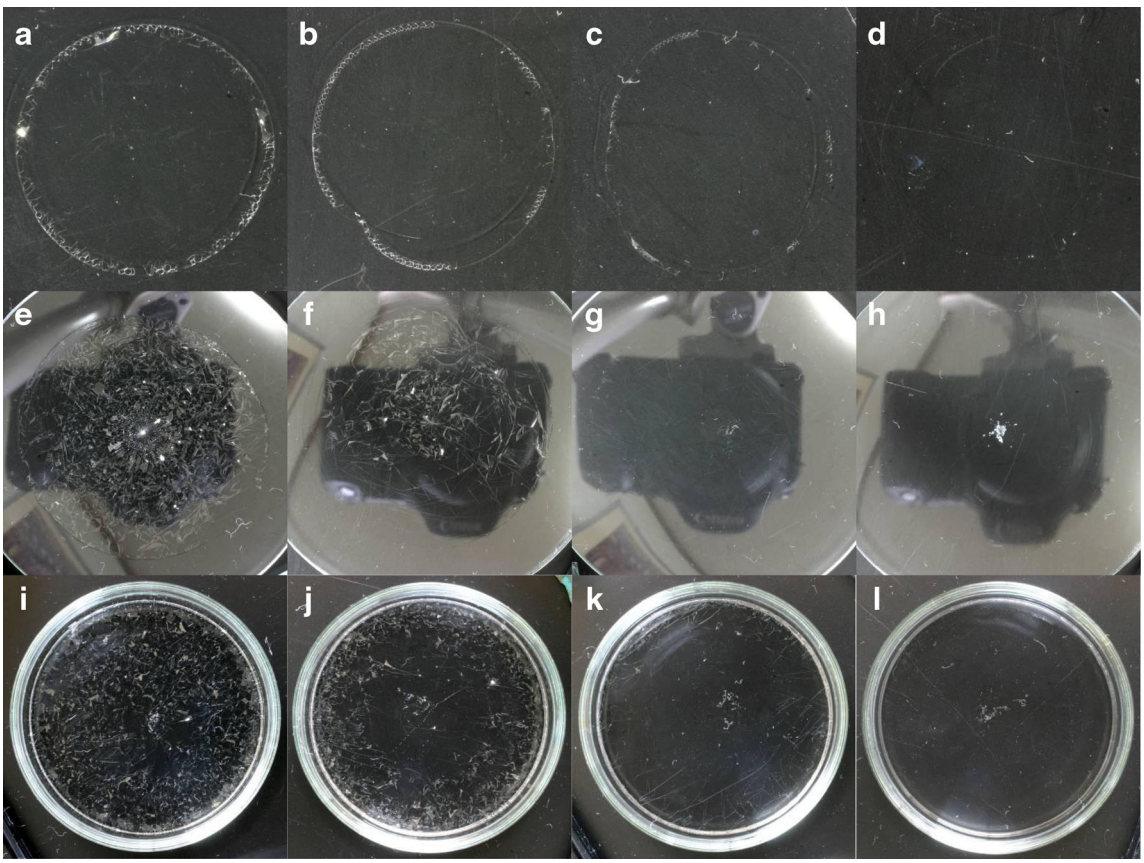

Fig. 1 Drying dissipative patterns of aqueous HPMA solution on a cover glass (**a**–**d**), a watch glass (**e**–**h**), and a glass dish (**i**–**l**) at 25 °C. 0.1 ml, **a**, **e**, **i** [HPMA]=0.1 monoM, **b**, **f**, **j** 0.05 monoM, **c**, **g**, **k** 0.02 monoM, **d**, **h**, **l** 0.0067 monoM

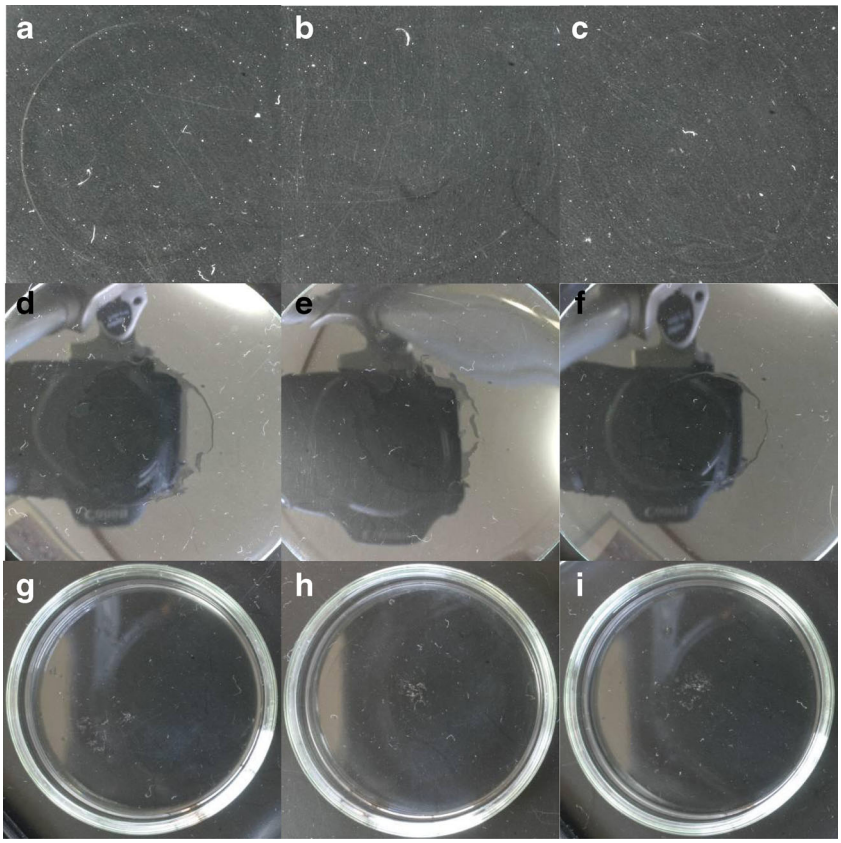

Fig. 2 Drying dissipative patterns of aqueous NaHPMA solution on a cover glass (**a**–**c**), a watch glass (**d**–**f**), and a glass dish (**g**–**i**) at 25 °C. 0.1 ml, **a**, **d**, **g** [NaHPMA]=0.095 monoM, **b**, **e**, **h** 0.048 monoM, **c**, **f**, **i** 0.025 monoM

concentrations. However, observation of the broad ring at 0.0067 monoM was not so easy with the naked eyes, where "monoM" indicates the polymer concentration given by the monomer units in moles per liter. The dried films of HPMA were weakly hygroscopic. Figure 2 shows typical examples of the close-up pictures of NaHPMA solutions on a cover glass (a–c), a watch glass (d–f), and a glass dish (g–i). The aqueous solutions of HPMA and NaHPMA were transparent, and any precipitation of the solid polymers was not observed throughout the drying processes in the liquid state. The dried films at room atmosphere were transparent and highly hygroscopic. Therefore, only the broad rings were recognized with the naked eyes. The images of camera are observed in the pictures of Figs. 1 and 2 on a watch glass, since the drying patterns are transparent and not observed so clearly. The hygroscopic strength was in the order NaPMA < HPMA < NaHPMA. The reason for observing the order in the hygroscopic strength is not clear yet. Main broad rings of HPMA formed at the outside edge irrespective of polymer concentration. Interestingly, simplified laurel crown type patterns appeared at high concentrations and on a cover glass (see pictures a and b). Simplified laurel crown patterns were observed clearly with a polarizing microscope as will be described below in Fig. 7 and supported the strong solute–substrate affinity. The laurel crown type ring is not so familiar. The patterns have been observed only for α-cyclodextrin, hitherto in the author's laboratory [45].

Figure 3 shows the d_f/d_i values of HPMA (circles), NaHPMA (triangles), and NaPMA (squares). Here, d_f and d_i are the sizes of the broad ring on the dried film and the initial liquid droplet in diameter, respectively. Open symbols show the values on a cover glass, and solid symbols are on a watch glass. For HPMA (open and solid circles), the broad rings formed at the outside edge and d_f/d_i were unity irrespective of polymer concentration. On the other hand, the d_f/d_i of NaHPMA and NaPMA decreased sharply at the lower polymer concentrations than the critical concentration, m^*. It is highly plausible that the d_f/d_i values of HPMA decrease from unity at the lower concentrations than 0.0005 monoM. These results in Fig. 3 support the fact that the single broad rings form and m^* values are in the order HPMA < NaPMA < NaHPMA.

Sharpness parameters of the broad ring, S and S', are evaluated from the thickness profiles and the widths of the broad rings, respectively. The S values are given by the ratio of film size in diameter (d_f) against the full width at half maximum ($FWHM$) in Eq. (1).

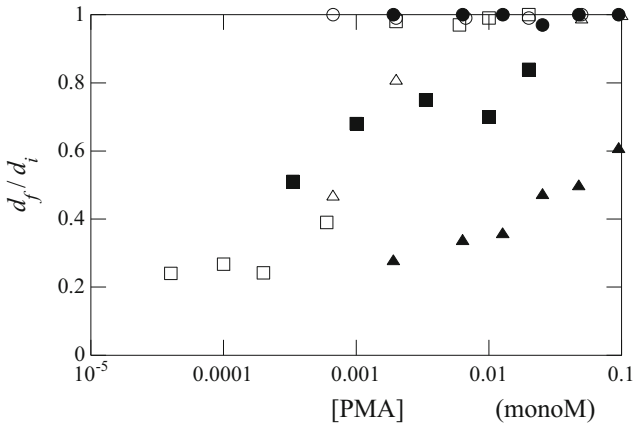

Fig. 3 Plots of d_f/d_i of HPMA, NaHPMA, and NaPMA on a cover glass (*circles*: HPMA, *triangles*: NaHPMA, *squares*: NaPMA) and a watch glass (*solid circles*: HPMA, *solid triangles*: NaHPMA, *solid squares*: NaPMA) at 25 °C

$$S = df/FWHM \tag{1}$$

When the thickness profile is normal distribution, *FWHM* is given by Eq. (2), where *s* is the corresponding standard deviation [50].

$$FWHM = 2.355\ \mathrm{s} \tag{2}$$

Another kind of sharpness parameter, *S′*, is also evaluated simply from the ratio of the dried film size against the width of the broad ring (*WBR*) observed macroscopically.

$$S' = (df/WBR) \times 2 \tag{3}$$

Here, *FWHM* is assumed to be half of *WBR*, i.e., the thickness profiles are approximated to be isosceles triangle-shaped.

Figure 4 shows the *S′* values of HPMA (circles), NaHPMA (crosses), and NaPMA (triangles) as a function of polymer concentration. For comparison, *S* and *S′* values of poly(ethylene glycol) (PEG20K) are also shown in square symbols [41]. The sharpness parameters of the broad rings were in the order NaPMA < NaHPMA ≦ HPMA. *S* (or S′) is one of the most convenient parameters showing the diffusivity of the solutes during the processes of convection. The magnitudes of *S* values of NaPMA were similar to those of PEG20K. Very high *S* values observed for HPMA are similar to those for coffee and black tea. The very strong solute–substrate affinity is deduced for HPMA, coffee, and black tea. In conclusion, all the polymers HPMA, NaHPMA, and NaPMA show the single type broad rings. Furthermore, very strong solute–substrate affinity exists for HPMA, whereas weak inter-solute and solute–substrate affinity is clear for NaHPMA and NaPMA. Recently, all the macroscopic broad rings observed hitherto were compiled into six groups from behaviors of d_f/d_i values and sharpness parameters as is shown in Table 1. HPMA, NaHPMA, and NaPMA are grouped into E, A, and A, respectively.

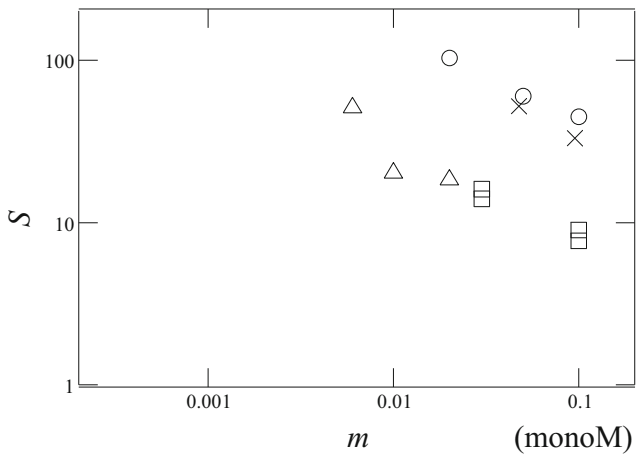

Fig. 4 Sharpness of the broad rings of HPMA (*circles*), NaHPMA (*crosses*), NaPMA (*triangles*), and PEG20K (*squares*) on a cover glass at 25 °C

Microscopic drying patterns of HPMA and NaHPMA solutions

Figures 5 and 6 show the typical microscopic drying patterns of HPMA on a cover glass (a–d), a watch glass (e–h), and a glass dish (i–l) at the polymer concentrations 0.1 monoM and 0.05 monoM, respectively. On a cover glass, very small inner broad ring appeared in addition to the main broad ring at the outside edge of the dried film. However, height of the inner rings is quite low compared with the ring at the outside edge. The inner rings will be safely neglected when the types of the drying patterns are assigned. Multiple fine rings were observed. The white-colored patterns in picture d of Figs. 5 and 6 are the simplified laurel crown patterns. The dried film on a cover glass substrate looks transparent and more hygroscopic compared with the films on a watch glass and a glass dish. On a watch glass, spoke-like patterns appeared clearly, and dispatch of the dried film from the substrate surface is clear in the figures. Number of spoke lines decreased sharply on a glass dish, and the dispatch is also clearly observed.

Figure 7 shows typical examples of the polarizing microscopic drying patterns of HPMA on a watch glass (a–c) and a cover glass (d). Very clear spoke-like cracks appeared around the central area on a watch glass. In picture c, arrayed pipes are recognized through the polarizing microscopy. Furthermore, very small and short rod-like blocks are observed whole the area of picture c. Assignment of these structures is not available yet at

Table 1 Six groups of macroscopic patterns appearing in the drying patterns and their relations with d_f/d_i and S values

Group	Broad ring (BR)	d_f/d_i	S	Affinitive interaction	Typical solutes
A	1BR	0~1, up with concentration	High	Weak inter-solutes, solute–substrate affinity	NaPMA, NaHPMA, polystyrene-, silica-PEG, PLHBr, rhodamine 6G, uranine
B	2BR (outside) (inner)	1	High	Strong solute–substrate affinity and weak inter-solute affinity	PMMA spheres, NaPGA, CD1
		0~1, up with concentration	Low		NaCMC, NaDSS, HPC, CD, pNIPAm, lpNIPAm, (μ)PEGMA-P2VP spheres
C	2BR (outside) (inner)	1	High	Strong solute–substrate affinity and strong inter-solute affinity	pNIPAm (70-5), CAIBA-P2VP, AIBA-P2VP spheres
		0~1, down with concentration	Low		KPolyA, KPolyA + KPolyU
D	1BR	<0.1, down with concentration or keep constant	Low	Very strong inter-solute affinity and weak solute–substrate affinity	NaHLA, NaDNA
D′	1BR	0.25~0.5 up with concentration	–	Strong inter-solute affinity and weak solute–substrate affinity	NaCl, KCl, $CaCl_2$, $LaCl_3$
E	1BR	1	High	Very strong solute–substrate affinity during solidification	HPMA, coffee, black tea
F	Central round hill (or +1BR (outside))	0 (1)	Very low (<10)	Associated non-spherical solutes, structured solutes	Bentonite, tungstic acid, PGK, gelatin, ARS, PBA spheres, POE5C18

PLHBr poly(lysine hydrobromide), *PMMA* poly(methyl methacrylate), *NaPGA* sodium salt of poly(α-glutamic acid), *CD1* colloidal diamond particles, *NaCMC* sodium salt of carboxymethyl cellulose, *NaDSS* sodium salt of dextran sulfate, *HPC* hydroxypropyl cellulose, *CD* cyclodextrin, *pNIPAm* poly(*N*-isopropyl acrylamide) sphere, *lpNIPAm* linear-type poly(*N*-isopropyl acrylamide), *μPEGMA-P2VP* micrometer-sized poly(2-*N*-vinylpyridine) gel sphere, *CAIBA-P2VP, AIBA-P2VP* poly(2-*N*-vinylpyridine) gel spheres, *NaHLA* sodium salt of hyaluronic acid, *PGK* palygorskite particle, *ARS* arrow-root starch, *PBA* poly(*n*-butyl acrylate), *POE5C18* polyoxyethylene(5)-*n*-stearyl ether

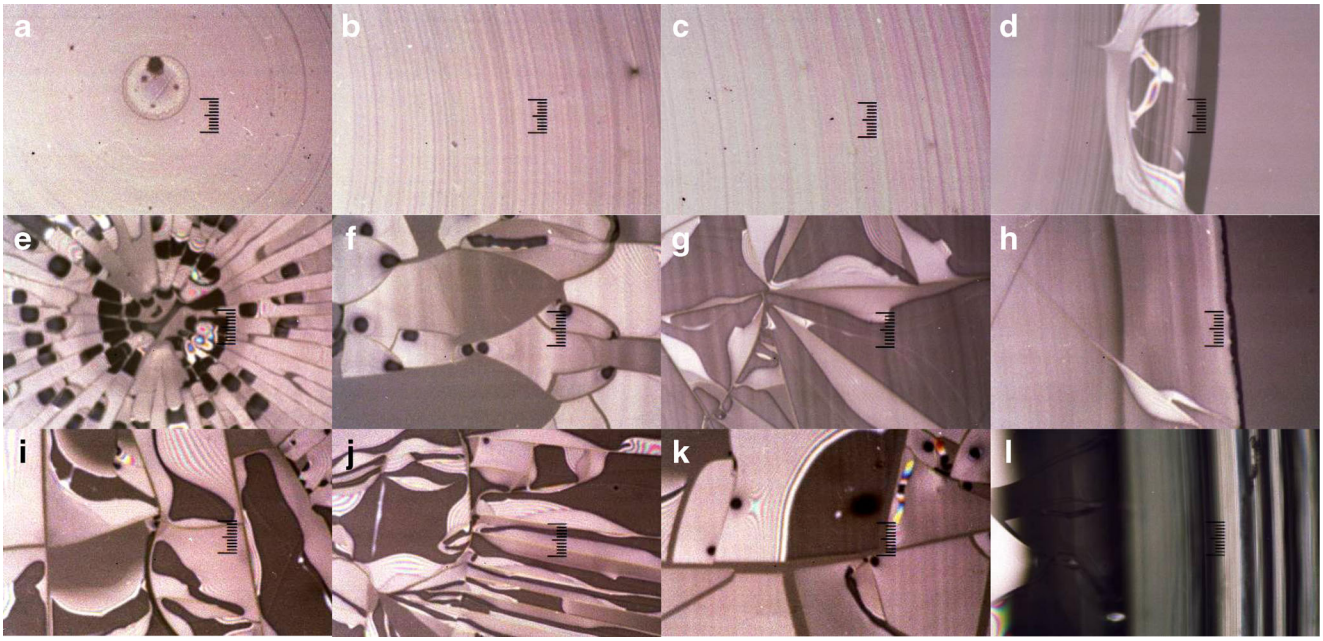

Fig. 5 Microscopic drying patterns of aqueous HPMA solution on a cover glass (**a**–**d**), a watch glass (**e**–**h**), and a glass dish (**i**–**l**) at 25 °C. [HPMA]=0.1 monoM, **a**, **e**, **f** to **d**, **h**, **l** are the pictures from the *center* to the *right*, full scales are 200 μm

present. There seems to form some primitive organized single crystals.

Figure 8 shows typical examples of the microscopic drying patterns of NaHPMA at 0.095 monoM on a cover glass (a–d), a watch glass (e–h), and a glass dish (i–l) from the center (a, e, i) to the right-hand side outside edge of the dried film (d, h, l). For NaPMA samples, clear-cut spherulite and/or hedrite crystals appeared, and the dissipative crystallization coupled with the broad ring patterns [42]. However, any dissipative crystallization phenomenon was not observed for HPMA and NaHPMA. Main causes for these observations are undoubtedly due to the hygroscopic properties of HPMA and NaHPMA.

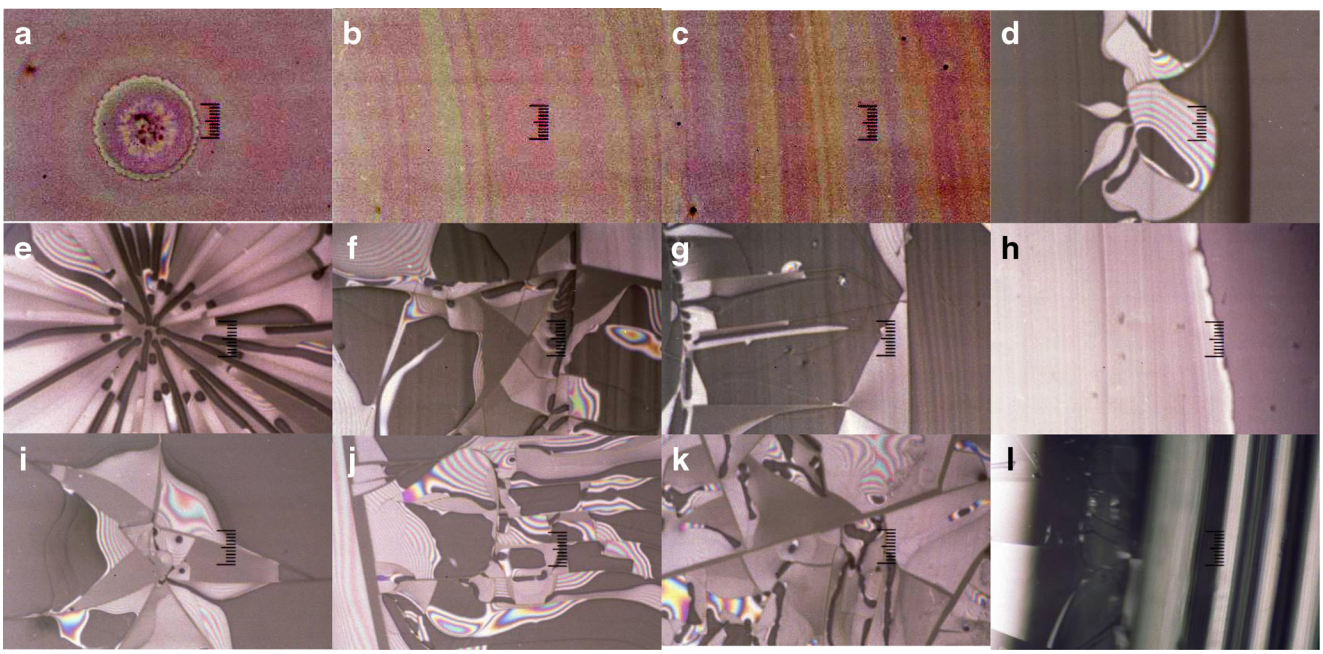

Fig. 6 Microscopic drying patterns of aqueous HPMA solution on a cover glass (**a**–**d**), a watch glass (**e**–**h**), and a glass dish (**i**–**l**) at 25 °C. [HPMA]=0.05 monoM, **a**, **e**, **f** to **d**, **h**, **l** are the pictures from the *center* to the *right*, full scales are 200 μm

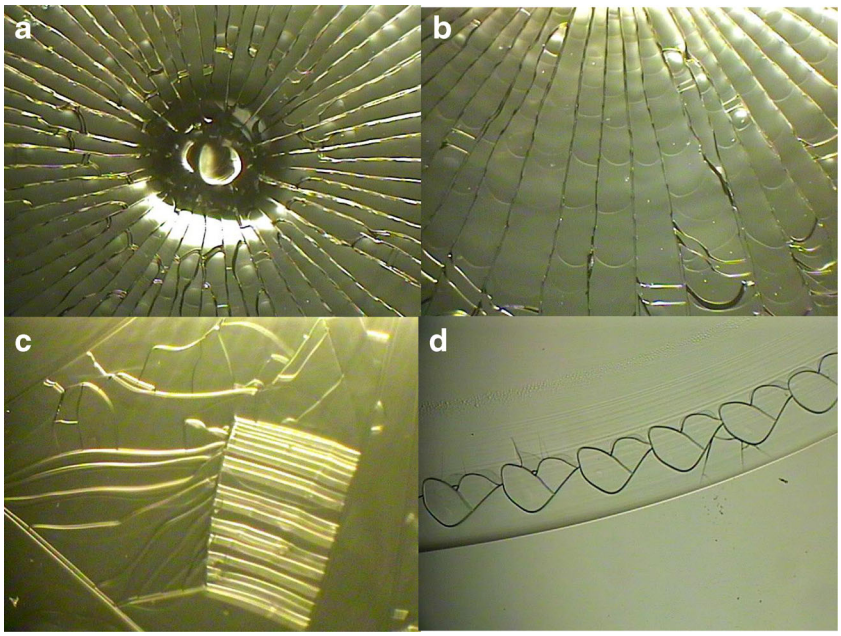

Fig. 7 Polarizing microscopic drying patterns of HPMA on a watch glass (**a**, **b**, **c**) and a cover glass (**d**). **a**, **b**, **c** [HPMA]=0.1 monoM, **d** 0.05 monoM, *lengths* of the picture frame are 2.6 mm× 3.4 mm

Concluding remarks

In this work, drying dissipative patterns of aqueous solutions of HPMA and NaHPMA were studied on a cover glass, a watch glass, and a glass dish on macroscopic and microscopic scales. Several important results were obtained. Firstly, HPMA and NaHPMA are highly hygroscopic, and observation of the microscopic structures was very difficult. Secondarily, the broad rings were single type for HPMA, NaHPMA, and NaPMA. Very strong solute–substrate and inter-solute affinities were deduced from the d_f/d_i values and the sharpness parameters of the broad ring. For NaHPMA and NaPMA, rather weak solute–substrate and inter-solute affinities were deduced. Observation of macroscopic and microscopic structures in a dry box that coexisted with desiccant is highly interesting in the future, though the experiments are not so easy.

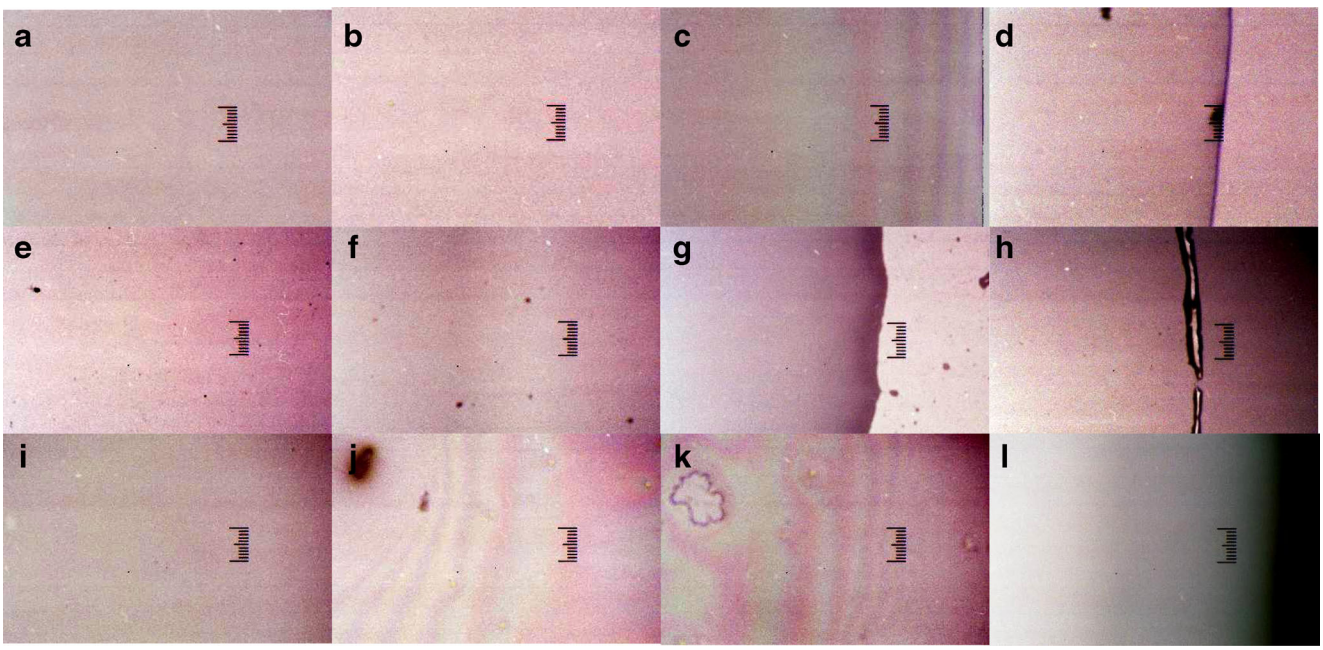

Fig. 8 Microscopic drying patterns of aqueous NaHPMA solution on a cover glass (**a**–**d**), a watch glass (**e**–**h**) and a glass dish (**i**–**l**) at 25 °C. [NaHPMA]=0.095 monoM, **a**, **e**, **f** to **d**, **h**, **l** are the pictures from the *center* to the *right*, full scales are 100 μm (**a**–**d**, **i**–**l**) and 200 mm (**e**–**h**)

References

1. Okubo T (2006) Drying dissipative structures of colloidal dispersions. In: Stoylov SP, Stoimenova MV (eds) Molecular and colloidal electro-optics. CRC Book,Taylor & Francis, pp573–589
2. Okubo T (2008) Convectional, sedimentation and drying dissipative patterns of colloidal dispersions and solutions. In: Nagarajan R, Hatton TA (eds) Nanoparticles: syntheses, stabilization, passivation and functionalization. ACS Book, Washington DC, p 256
3. Okubo T (2001) Beautiful world of colloids and interfaces. Matsuo Press, Gifu **(Japanese)**
4. Okubo T (2010) Dissipative structure in the course of drying suspensions and solutions. Macromol Symp 288:67–77
5. Okubo T, Kanayama S, Ogawa H, Hibino M, Kimura K (2004) Dissipative structures formed in the course of drying the aqueous solution of poly(allylamine hydrochloride) on a cover glass. Colloid Polym Sci 282:230–235
6. Okubo T, Shinoda C, Kimura K, Tsuchida A (2005) Drying dissipative structures of non-ionic surfactants in aqueous solution. Langmuir 21:9889–9895
7. Okubo T, Kanayama S, Kimura K (2004) Dissipative structures formed in the course of drying the aqueous solution of *n*-dodecyltrimethylammonium chloride on a cover glass. Colloid Polym Sci 282:486–494
8. Gribbin G (1999) Almost everyone's guide to science. The universe, life and everything. Yale University Press, New Haven
9. Ball P (1999) The self-made tapestry. Pattern formation in nature. Oxford Univ Press, Oxford
10. Terada T, Yamamoto R, Watanabe T (1934) Experimental studies on colloid nature of Chinese black ink. Part. 1.Sci Paper Inst Phys Chem Res Jpn 23:173–184
11. Terada T, Yamamoto R, Watanabe T (1934) Experimental studies on colloid nature of Chinese black ink. Part. 2.Sci Paper Inst Phys Chem Res Jpn 27:75–92
12. Terada T, Yamamoto R (1935) Proc Imper Acad Tokyo 11:214
13. Nakaya U (1947) Memoirs of Torahiko Terada. Kobunsya, Tokyo **(Japanese)**
14. Okubo T, Kimura H, Kimura T, Hayakawa F, Shibata T, Kimura K (2005) Drying dissipative structures of Chinese black ink on a cover glass and in a dish. Colloid Polym Sci 283:1–9
15. Okubo T (2006) Convectional, sedimentation and drying dissipative structures of ethanol suspension of colloidal silica (110 nm in diameter) spheres. Colloid Polym Sci 285:225–231
16. Okubo T (2009) Convectional and sedimentation dissipative patterns of Miso-soup. Colloid Polym Sci 287:167–178
17. Okubo T, Okamoto J, Tsuchida A (2009) Convectional, sedimentation and drying dissipative patterns of coffee in the presence of cream and in its absence. Colloid Polym Sci 287:351–365
18. Okubo T, Okamoto J, Tsuchida A (2009) Convectional, sedimentation and drying dissipative patterns of black tea in the presence of cream and in its absence. Colloid Polym Sci 287:645–657
19. Okubo T, Okamoto J, Tsuchida A (2008) Convectional, sedimentation and drying dissipative patterns of colloidal crystals of poly(methyl methacrylate) on a cover glass. Colloid Polym Sci 286:1123–1133
20. Okubo T (2008) Convectional, sedimentation and drying dissipative patterns of colloidal crystals of poly(methyl methacrylate) spheres on a watch glass. Colloid Polym Sci 286:1307–1315
21. Okubo T (2008) Convectional, sedimentation and drying dissipative patterns of colloidal silica (183 nm in diameter) suspension in a glass dish and a watch glass. Colloid Polym Sci 286:1411–1423
22. Yamaguchi T, Kimura K, Tsuchida A, Okubo T, Matsumoto M (2005) Drying dissipative structures of the aqueous suspensions of monodispersed bentonite particles. Colloid Polym Sci 283: 1123–1130
23. Okubo T (2006) Sedimentation and drying dissipative structures of colloidal silica (1.2 μm in diameter) suspensions in a watch glass. Colloid Polym Sci 284:1191–1196
24. Okubo T (2006) Sedimentation and drying dissipative structures of colloidal silica (1.2 mm in diameter) suspensions in a glass dish and a polystyrene dish. Colloid Polym Sci 284:1395–1401
25. Okubo T, Okamoto J, Tsuchida A (2007) Sedimentation and drying dissipative patterns of colloidal silica (305 nm in diameter) suspensions in a glass dish and a watch glass. Colloid Polym Sci 285:967–975
26. Okubo T (2007) Sedimentation and drying dissipative patterns of colloidal silica (560 nm in diameter) suspensions in a glass dish and a watch glass. Colloid Polym Sci 285:1495–1503
27. Okubo T, Okamoto J, Tsuchida A (2008) Sedimentation and drying dissipative patterns of binary suspensions of colloidal silica spheres having different sizes. Colloid Polym Sci 286: 385–394
28. Okubo T, Okamoto J, Tsuchida A (2008) Sedimentation and drying dissipative patterns of ternary suspensions of colloidal silica spheres having different sizes. Colloid Polym Sci 286:941–949
29. Okubo T (2006) Sedimentation and drying dissipative structures of green tea. Colloid Polym Sci 285:331–337
30. Vanderhoff JW, Bradford EB, Carrington WK (1973) The transport of water through latex films. J Polym Sci Polym Symp 41:155–174
31. Nicolis G, Prigogine I (1977) Self-organization in non-equilibrium systems. Wiley, New York
32. Ohara PC, Heath JR, Gelbart WM (1997) Bildung von Submikrometer-grossen Partikelringen beim Verdunsten Nanopartikel-haltiger Loesungen. Angew Chem 109:1120–1122
33. Maenosono S, Dushkin CD, Saita S, Yamaguchi Y (1999) Growth of a semi conductor nanoparticle ring during the drying of a suspension droplet. Langmuir 15:957–965
34. Nikoobakht B, Wang ZL, El-Sayed MA (2000) Self-assembly of gold nanorods. J Phys Chem B 104:8635–8640
35. Ung T, Litz-Marzan LM, Mulvaney P (2001) Optical properties of thin films of Au@SiO2 particles. J Phys Chem B 105:3441–3452
36. Okubo T, Onoshima D, Tsuchida A (2007) Drying dissipative patterns of biological polyelectrolyte solutions. Colloid Polym Sci 285:999–1007
37. Shimomura M, Sawadaishi T (2001) Bottom-up strategy of materials fabrication: a new trend in nanotechnology of soft materials. Curr Opin Coll Interf Sci 6:11–16
38. Okubo T, Yamada T, Kimura K, Tsuchida A (2006) Drying dissipative structures of aqueous solution of poly(ethylene glycol) on a cover glass. Colloid Polym Sci 284:396–404
39. Okubo T, Itoh E, Tsuchida A, Kokufuta E (2006) Drying dissipative structures of the thermosensitive gels of poly(*N*-isopropylacrylamide) on a cover glass. Colloid Polym Sci 285:339–349
40. Okubo T, Yokota N, Tsuchida A (2007) Drying dissipative patterns of dyes in ethylalcohol on a cover glass. Colloid Polym Sci 285: 1257–1265
41. Okubo T, Okamoto J, Takahashi S, Tsuchida A (2009) Drying dissipative structures of aqueous solution of poly(ethylene glycol) on a cover glass, a watch glass and a glass dish. Colloid Polym Sci 287:933–942
42. Okubo T, Hagiwara A, Kitano H, Okamoto J, Takahashi S, Tsuchida A (2009) Dissipative crystallization of aqueous solution of sodium polymethacrylate. Colloid Polym Sci 287:1155–1165
43. Okubo T, Takahashi S, Tsuchida A (2011) Dissipative crystallization of sodium salts of poly(D-glutamic acid), poly(L-glutamic acid) and their low molecular weight analogs. Colloid Polym Sci 289: 1729–1737
44. Okubo T, Okamoto J, Tsuchida A (2010) Dissipative crystallization of poly-D-lysine hydrobromide, poly-L-lysine hydrobromide and their low molecular weight analogs. Colloid Polym Sci 288:981–989

45. Okubo T (2013) Inclusional association as studied by the drying dissipative structure. Part 1. Drying patterns of α-, β- and γ-cyclodextrin. Colloid Polym Sci 291:2447–2454
46. Okubo T, Mizutani M, Takahashi S, Tsuchida A (2010) Dissipative crystallization of sodium salt of deoxyribonucleic acid. Colloid Polym Sci 288:1435–1444
47. Okubo T, Takahashi S, Tsuchida A (2011) Dissipative crystallization of potassium salt of poly(riboadenylic acid). Colloid Surf B Biointerf 87:11–17
48. Okubo T (2011) Dissipative crystallization of aqueous mixtures of potassium salts of poly(riboadenylic acid) and poly(ribouridylic acid). Colloid Surf B Biointerf 87:439–446
49. Okubo T (2014) Dissipative crystallization of aqueous mixtures of potassium salts of poly(riboguanylic acid) and poly(ribocytidylic acid). Colloid Polym Sci 292:1419–1427
50. Ida T (2008) New measures of sharpness for symmetric powder diffraction peak profiles. J Appl Crystallograph 41: 393–401